A novel acidotropic pH indicator and its potential application in labeling acidic organelles of live cells

Zhenjun Diwu, Chii-Shiarng Chen, Cailan Zhang, Dieter H Klaubert and Richard P Haugland

Background: Ratio imaging has received intensive attention in the past few decades. The growing potential of ratio imaging is significantly limited, however, by the lack of appropriate fluorescent probes, for acidic organelles in particular. The classic fluorescent dyes (such as fluoresceins, rhodamines and coumarins) are not suitable for studying acidic organelles (such as lysosomes) because their fluorescence is significantly decreased under neutral or acidic conditions. This has motivated us to develop probes that can be used in ratio imaging that are strongly fluorescent even in acidic media.

Results: The compound 2-(4-pyridyl)-5-((4-(2-dimethylaminoethyl-aminocarbamoyl)methoxy)phenyl)oxazole (PDMPO) was prepared and characterized as a new acidotropic dual-excitation and dual-emission pH indicator. It emits intense yellow fluorescence at lower pH and gives intense blue fluorescence at higher pH. This unique pH-dependent fluorescence property was readily explored to selectively stain lysosomes and to determine the pH of the organelle in an emission-ratio-imaging mode. PDMPO is selectively localized to lysosomes and exhibits a pH-dependent dual excitation and emission.

Conclusions: PDMPO selectively labels acidic organelles (such as lysosomes) of live cells and the two distinct emission peaks can be used to monitor the pH fluctuations of live cells in ratio measurements. Additionally, the very large Stokes shift and excellent photostability of PDMPO make the compound an ideal fluorescent acidotropic probe. The unique fluorescence properties of PDMPO might give researchers a new tool with which to study acidic organelles of live cells.

Address: Molecular Probes, Incorporated, 4849 Pitchford Avenue, Eugene, Oregon 97402, USA.

Correspondence: Zhenjun Diwu
E-mail: zhenjun@probes.com

Key words: acidic organelles, fluorescence, lysosome, pH indicator, ratio imaging

Received: **2 November 1998**
Revisions requested: **27 November 1998**
Revisions received: **16 March 1999**
Accepted: **25 March 1999**

Published: **4 June 1999**

Chemistry & Biology July 1999, **6**:411–418
http://biomednet.com/elecref/1074552100600411

Introduction

Intracellular pH plays an important role in many cellular events such as cell growth [1], calcium regulation [2,3], endocytosis [4], chemotaxis [5], cell adhesion [6], and other cellular processes [7–10]. Both invasive methods such as microelectrodes, and noninvasive techniques such as nuclear magnetic resonance (NMR), absorption and fluorescence spectroscopy have been used to measure intracellular pH. Because fluorescence spectroscopy provides greater sensitivity and is more convenient than other methods, fluorescent pH indicators have been widely applied in recent years to monitor changes in intracellular pH [11]. Among the dyes most commonly used for this purpose are 1,4-dihydroxyphthalonitrile (1,4-DHPN) [7], 8-hydroxypyrene-1,3,6-trisulfonic acid (HPTS) [12], 5-(and-6)-carboxyfluorescein [7], 4′,5′-dimethyl-5-(and-6)-carboxyfluorescein [7], 2′,7′-*bis*-(2-carboxyethyl)-5-(and-6)-carboxyfluorescein (BCECF) [7,13–15], carboxy-seminaphthofluoresceins (SNAFL®) [16] and carboxy-seminaphthorhodafluoresceins (SNARF®) [16]. Recently, green fluorescent protein (GFP) has also been used as an intracellular pH probe [17]. These existing pH probes are ill-adapted to study acidic organelles such as lysosomes, endosomes and spermatazoa acrosomes, however, not only because they do not selectively accumulate in acidic organelles but also because their fluorescence is greatly reduced in acidic media. Additionally, most of the existing intracellular pH indicators show a change in emission intensity with little or no changes in emission wavelength or band shape. The latter precludes pH determination by emission ratio measurements, although some intracellular pH indicators (such as BCECF) have been used in excitation ratio measurements [18].

It has been proven that pH plays a pivotal role in many acidic cellular compartments and that the monitoring of pH fluctuations in acidic organelles is essential to investigate the cellular functions of the compartments [12,19–21]. This has motivated us to develop a new fluorescent pH indicator that has a pK_a value close to the typical pH range of acidic organelles, and is more fluorescent in the acidic pH range than are conventional pH

Figure 1

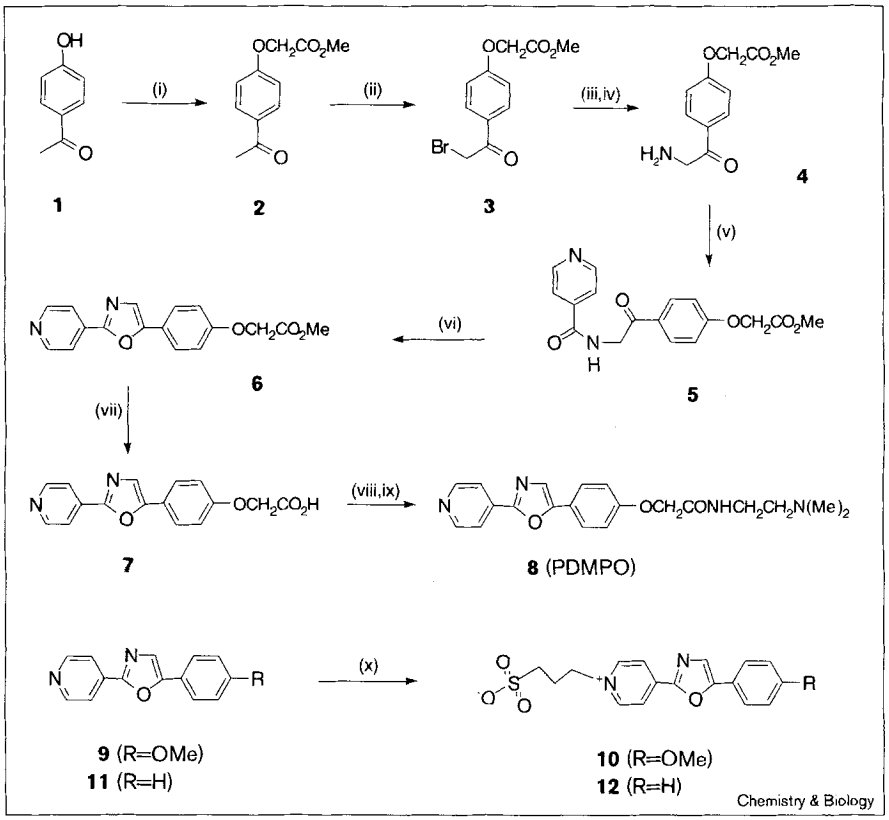

Syntheses and structures of PDMPO and related compounds. (i) Methyl bromoacetate/K_2CO_3/acetone, 95%; (ii) $CuBr_2$/ethyl acetate, 75%; (iii) hexamethylene-tetramine/$CHCl_3$, 98%; (iv) concentrated HCl, 87%; (v) isonicotinoyl chloride hydrochloride/pyridine/CH_2Cl_2, 91%; (vi) concentrated sulfuric acid, 94%; (vii) NaOH/MeOH, 91%; (viii) *N*-hydroxysuccinimide/DCC/DMF; (ix) *N,N*-dimethylethylenediamine, 85% (the combined yield with step (vii)); (x) 1,3-propane sultone/1,2-dichlorobenzene, 91%.

indicators. The probe should also preferably accumulate in acidic organelles of living cells.

We noted the unique intramolecular electron-transfer property of 2,5-diphenyloxazole systems when we developed the Dapoxyl™ dyes, a new type of environment-sensitive fluorescent molecule [22]. This property was further explored to develop 2-(4-pyridyl)-5-((4-(2-dimethylaminoethylaminocarbamoyl)methoxy)phenyl)oxazole (PDMPO), a pyridyl oxazole dye currently called 'Lysosensor™ Yellow/Blue'. This probe selectively accumulates in acidic organelles such as lysosomes, most probably through the protonation of the pyridyl and alkyl amino sidechain, and the protonated species emits intense yellow fluorescence that is presumably because of the protonation-induced intramolecular electron transfer of the pyridyl oxazole fluorophore.

Results and discussion

Synthesis

PDMPO was synthesized as outlined in Figure 1. Phenol **1** was readily alkylated with methyl bromoacetate to give acetophenone **2**, which was selectively converted into phenacyl bromide **3** via $CuBr_2$ bromination [23]. Compound **3** was converted into compound **4** via its hexamethylenetetraammonium salt. The aminoacetophenone was then condensed with isonicotinoyl chloride **2** to give amide **5** nearly quantitatively. Compound **5** was cyclized to give an excellent yield of oxazole **6** in concentrated sulfuric acid at room temperature. We found that sulfuric acid was the best dehydrating agent for the cyclization out of the many dehydrating agents tried including phosphorus oxychloride, acetic anhydride, methanesulfonic acid and dicyclohexylcarbodiimide. Compound **6** was hydrolyzed with sodium hydroxide and then coupled with *N,N*-dimethylethylenediamine to give PDMPO (compound **8**).

Absorption and fluorescence spectra

The absorption and fluorescence spectra of PDMPO were compared with those of compounds **9–12** and 2,5-diphenyloxazole (DPO) (Figure 2). The photophysical properties of the compounds are summarized in Table 1. As seen in Figure 2, PDMPO shows two distinct pH-dependent peaks in both excitation (with an isosbestic point at 359 nm) and fluorescence (with an isosbestic point at 495 nm) spectra. Both the absorption and fluorescence spectra of the protonated PDMPO are considerably red-shifted and broadened relative to those of the free base as seen in the Figure 2 and Table 1. Additionally, the absorption and fluorescence spectra of the protonated PDMPO resemble those of pyridinium oxazole **10**, whereas the absorption and fluorescence spectra of the

Figure 2

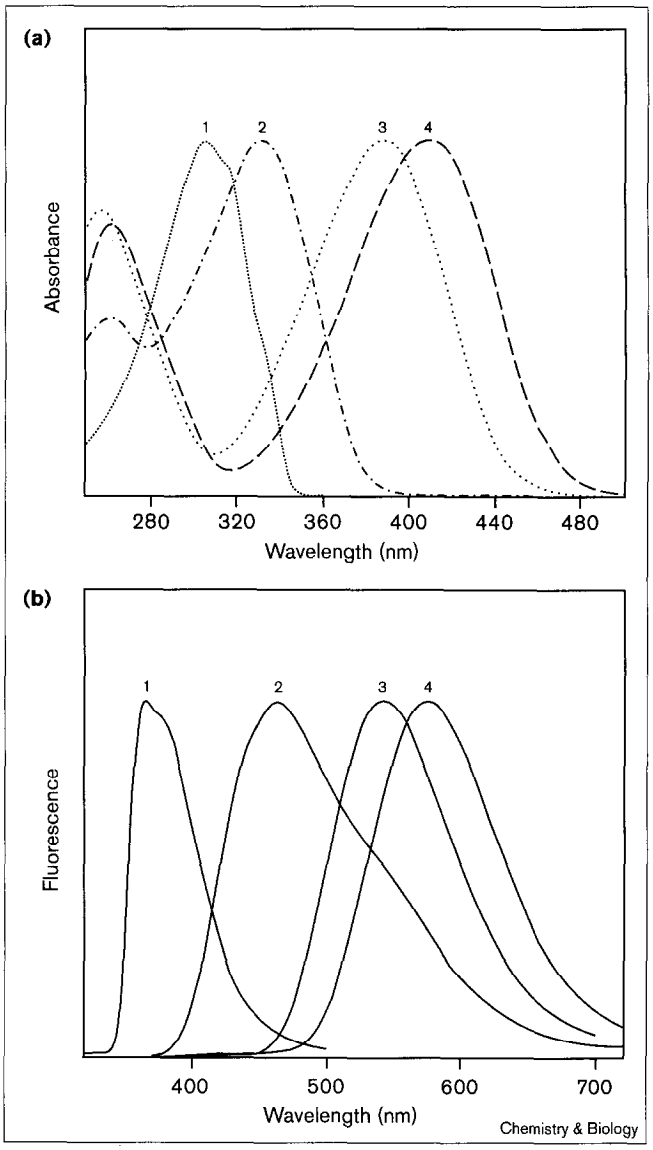

(a) The normalized absorption spectra of compounds **8** (PDMPO), **10** and DPO. The sample concentrations are 1–5 μM. Spectrum 1 is DPO in 1:1 water/methanol; spectrum 2 is compound **8** in water (pH 14.0); spectrum 3 is compound **8** in water (pH 1.0) and spectrum 4 is compound **10** in 1:1 water/methanol. **(b)** The normalized fluorescence spectra of compounds **8**, **10** and DPO. The sample concentrations are 1–5 μM. Spectrum 1 is DPO in 1:1 water:methanol; spectrum 2 is compound **8** in water (pH 14.0); spectrum 3 is compound **8** in water (pH 1.0) and spectrum 4 is compound **10** in 1:1 water:methanol.

free base are similar to those of compound **11** and DPO. Oxazole **10** embodies a strong electron-donating group (alkoxy) at position 4 of the 5-phenyl ring and a strong electron-withdrawing group (pyridinium) at position 2, forming a 'push–pull' electron transfer system from the 5-phenyl moiety to the 2-pyridium ring as observed with the Dapoxyl™ dyes [22]. In contrast, compound **11** and DPO lack such a 'push–pull' electron-transfer system.

Table 1

Spectral properties of compound 8 (PDMPO) and related compounds.

Compound	Solvent	$^*\lambda_{max}$ (nm)	$^\dagger\lambda_{max}$ (nm)	Φ_F	Stokes shift (nm)
8	Water (pH 1.0)	385	542	0.43	157
8	1:1 Water/methanol	330	442	0.69	112
8	Water (pH 14.0)	329	464	0.41	135
9	Water (pH 1.0)	386	544	0.46	158
9	1:1 Water/methanol	331	443	0.72	112
9	Water (pH 14.0)	329	465	0.42	136
10	1:1 Water/methanol	406	575	0.47	169
11	Water (pH 1.0)	364	476	0.98	112
11	1:1 Water/methanol	317	405	0.84	88
11	Water (pH 14.0)	316	410	0.80	94
12	1:1 Water/methanol	373	480	0.96	107
DPO	1:1 Water/methanol	305	366	0.99	61

$^*\lambda_{max}$, $^\dagger\lambda_{max}$ and Φ_F are absorption and fluorescence maxima, and fluorescence quantum yield respectively.

These facts imply that the observed longer wavelengths of absorption and fluorescence peaks of PDMPO might result from the transition of protonation-induced intramolecular charge transfer involving the alkoxy group (donor) and the pyridinium moiety (acceptor).

Compounds **9–12** and DPO were compared side by side to study the effect of a sidechain on the fluorescence of PDMPO and the results are summarized in Table 1. The similar spectral properties of PDMPO and compound **9** indicate that the sidechain does not exert a significant effect on the fluorescence although some aliphatic amino sidechains are known to quench the fluorescence of their host fluorophores via photo-induced electron transfer [24]. The relatively pH-insensitive absorption and fluorescence properties of compounds **10** and **12** suggests that protonation of the oxazole moiety is less likely than that of the pyridine ring and has minimal effect on the fluorescence under physiological pH conditions.

Unlike other fluorescent pH probes (such as fluoresceins and rhodamines) of which fluorescence is strongly quenched at lower pH, PDMPO still exhibits strong fluorescence at low pH at a constant dye concentration, as seen in Figure 3. Similar fluorescence behavior was also observed for compounds **9** and **11**. This unique pH dependence can be readily explored to develop fluorescent acidotropic probes such as PDMPO. The large Stokes shift and excellent photostability of the protonated species make the sensor a sensitive probe for acidic organelles.

It was observed that the fluorescence of PDMPO is relatively insensitive to the ionic strength of aqueous solutions. In either the presence or absence of 0.1 M NaCl or KCl (typical intracellular Na^+, K^+ and Cl^- concentrations), little change in the emission wavelengths or intensity

Figure 3

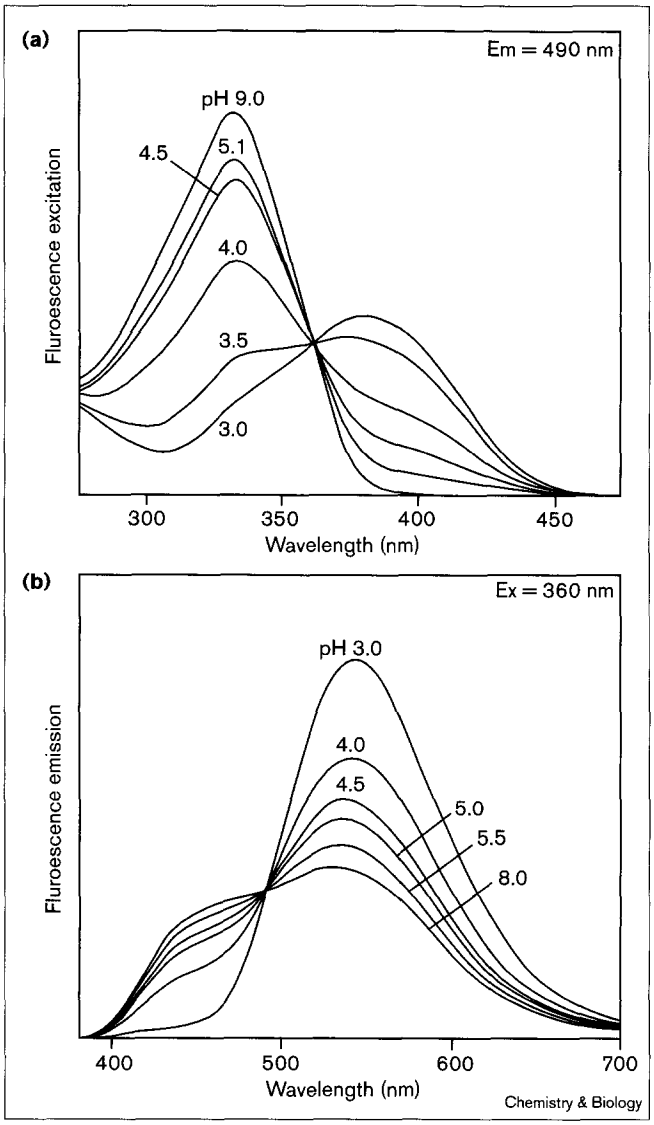

The pH-dependent electronic spectra of compound **8** at 1 μM. **(a)** Fluorescence excitation spectra at 490 nm emission and **(b)** fluorescence emission spectra at 360 nm excitation.

ratios was observed. Other halogen ions (such as Br^- and I^-) and cationic ions (such as 5 Mg^{2+} and 5 mM Ca^{2+}) have no significant effects either, although the fluorescence of most quinolium dyes is quenched by halogen ions [8].

pK_a value

For our particular application, we were only interested in the pK_a of the pyridyl moiety. As discussed above, only the protonation of the pyridyl moiety has substantial effect on the fluorescence of PDMPO. The p*K*a of PDMPO was therefore obtained by linear regression analysis of absorption spectral data to fit the following equation [25]:

$$pH = pK_a + c \times \log[(R-R_{min})/(R_{max}-R)] + \log (I^a/I^b) \quad (1)$$

where c is the slope, the pK_a of the dye is the intercept and R is the ratio of absorption, excitation or emission intensity at two wavelengths, with maximum and minimum limiting values of R_{max} and R_{min}, respectively. I^a/I^b is the ratio of absorption, excitation, or emission intensity in acid to the intensity in base at the wavelength chosen for the denominator of R. In the absence of competing equilibria, this correction vanishes at exact isosbestic wavelengths. In general, plots of R against pH showed clear plateaus and the limiting values (R_{max} and R_{min}) were determined by visual inspection of the titration curves.

Using absorption spectra, the pK_a of PDMPO (ground state) was determined to be 4.47 under our assay conditions [25], which is near to the typical pH range of acidic organelles such as lysosomes [20]. The pK_a of the ground state (obtained from the absorption spectra) is similar to the apparent pK_a value seen from the excitation spectra (see Figure 3a), but is different from the one derived from the emission spectra (see Figure 3b). This might be because emission spectra are generally used to calculate the pK_a of the excited state in the case of pyridine moiety [25]. This makes PDMPO useful for pH measurements in acidic organelles. PDMPO can be used to measure pH of lysosomes up to pH 6.0 in an emission ratio mode as shown in Figures 4 and 5. Because of its low pK_a values PDMPO has predominantly yellow fluorescence in acidic media (pH < 5.0) and blue fluorescence in less acidic organelles (pH > 6.0).

Lysosomal staining and ratiometric measurement of lysosomal pH

Lysosomes are typical acidic organelles and many probes have been developed to study the cellular compartment [20,21,26]. For example, some pyranine and fluorescein derivatives have been used to measure pH fluctuations in lysosomes [12,27]. Additionally, *N*-3-((2,4-dinitrophenyl)-amino)propylmethylamine (DAMP) has been used widely to label lysosomes. Unfortunately, DAMP is not fluorescent and must therefore be used in conjunction with anti-2,4-dinitrophenyl (DMP) antibodies conjugated to a fluorophore, enzyme or ferritin in order to visualize the staining pattern [8,21]. This tedious procedure has limited the application of DAMP for live cells.

As shown in Figure 1, PDMPO contains a weakly basic amino sidechain that mimics DMAP and chloroquine, the typical lysotropic agents, and selectively retains the compound in lysosomes presumably via the pH gradient of lysosomes [26]. We confirmed the utility of PDMPO for labeling lysosomes using a double-staining experiment with Madin Derby canine kidney (MDCK) cells. The

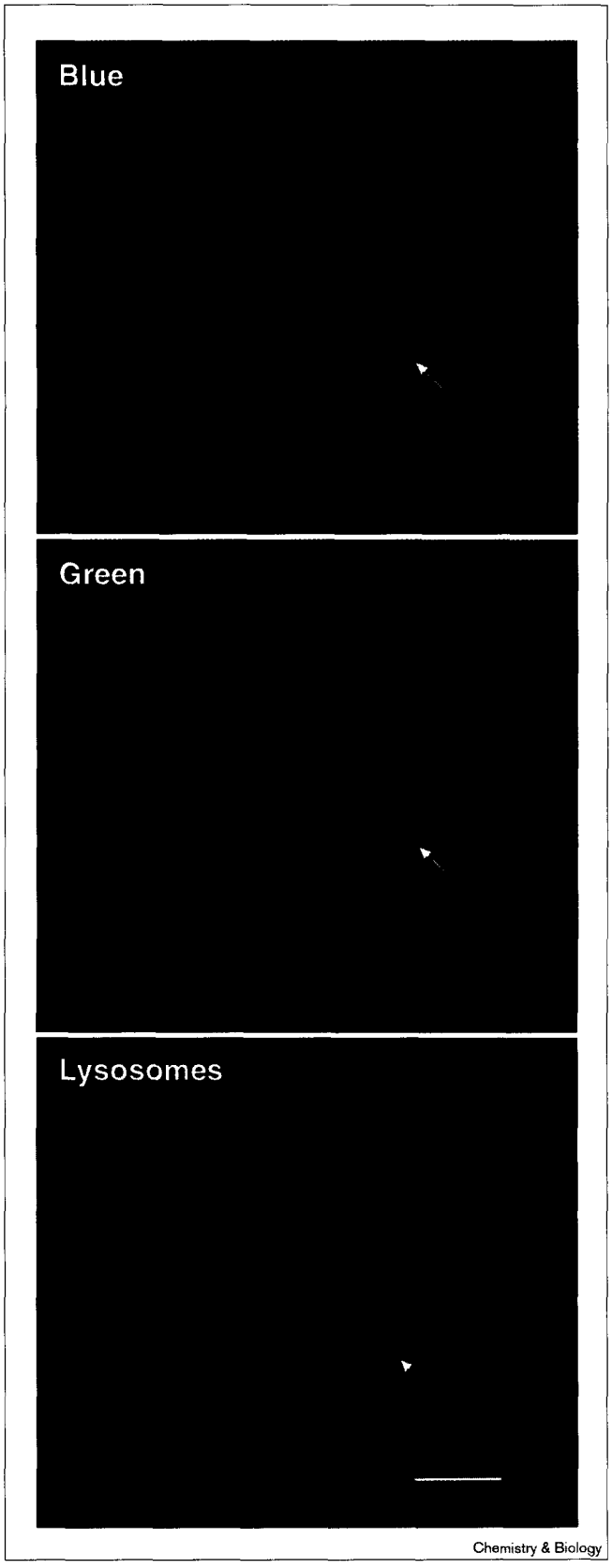

Figure 4

The accumulation of compound **8** in lysosomes. Lysosomes of MDCK cells were first labeled with Texas-Red-conjugated dextran, and then incubated with 5 μM compound **8** at 37°C for 5 min. Fluorescence images of compound-**8**-stained cells (blue and green) and Texas-Red-dextran-stained cells were acquired using the appropriate filter sets as described as in the Materials and methods section. As indicated by the arrow, compound **8** is selectively distributed in lysosomes and co-localized with the fluorescent dextran. Scale bar, 10 μm.

cells were first treated with Texas-Red-conjugated dextran to label the lysosomal population and were then stained with PDMPO. The fluorescence images of the PDMPO-stained cells ('blue' and 'green') and Texas-Red-dextran-stained cells were acquired using the appropriate filter sets as described as in the Materials and methods section. As shown in Figure 4, PDMPO specifically distributed in lysosomes where it is well co-localized with Texas Red dextran (red fluorescence). Under our experimental conditions we did not observe staining of other acidic organelles (such as the Golgi apparatus). It has been shown previously that the red fluorescent dextran is internalized into cells through endocytic pathway, and eventually transported to and accumulated in lysosomes [28].

As shown in Figures 5 and 6, the new sensor can be readily used to monitor the lysosomal pH of live cells in an emission-ratiometric mode. The fluorescence intensity ratio of

Figure 5

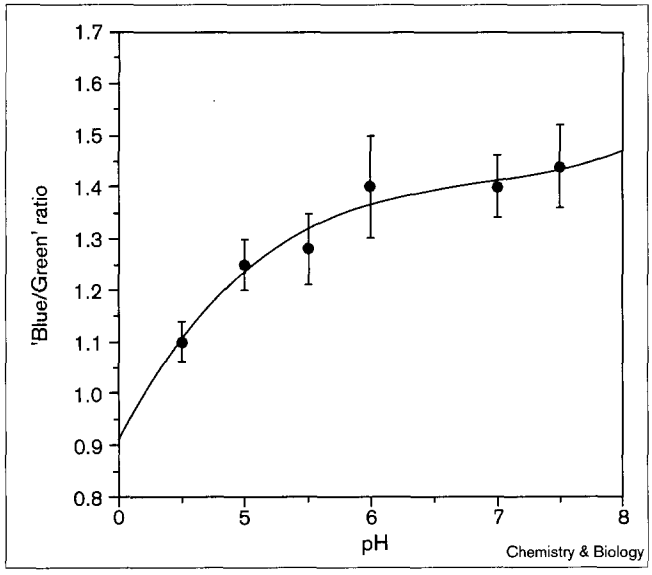

Standard pH calibration curve of compound **8** ('blue'/'green' emission ratio against pH). Live MDCK cells were stained with compound **8** and then incubated with MES calibration buffer solutions (pH from 4.0 to 7.5) containing nigericin and monensin. Blue and green images of total lysosomal population in the same cell were acquired as described in the Materials and methods section. The ratio of blue and green fluorescence intensity in the lysosomes was then calculated according to the procedure of Chen *et al.* [37].

Figure 6

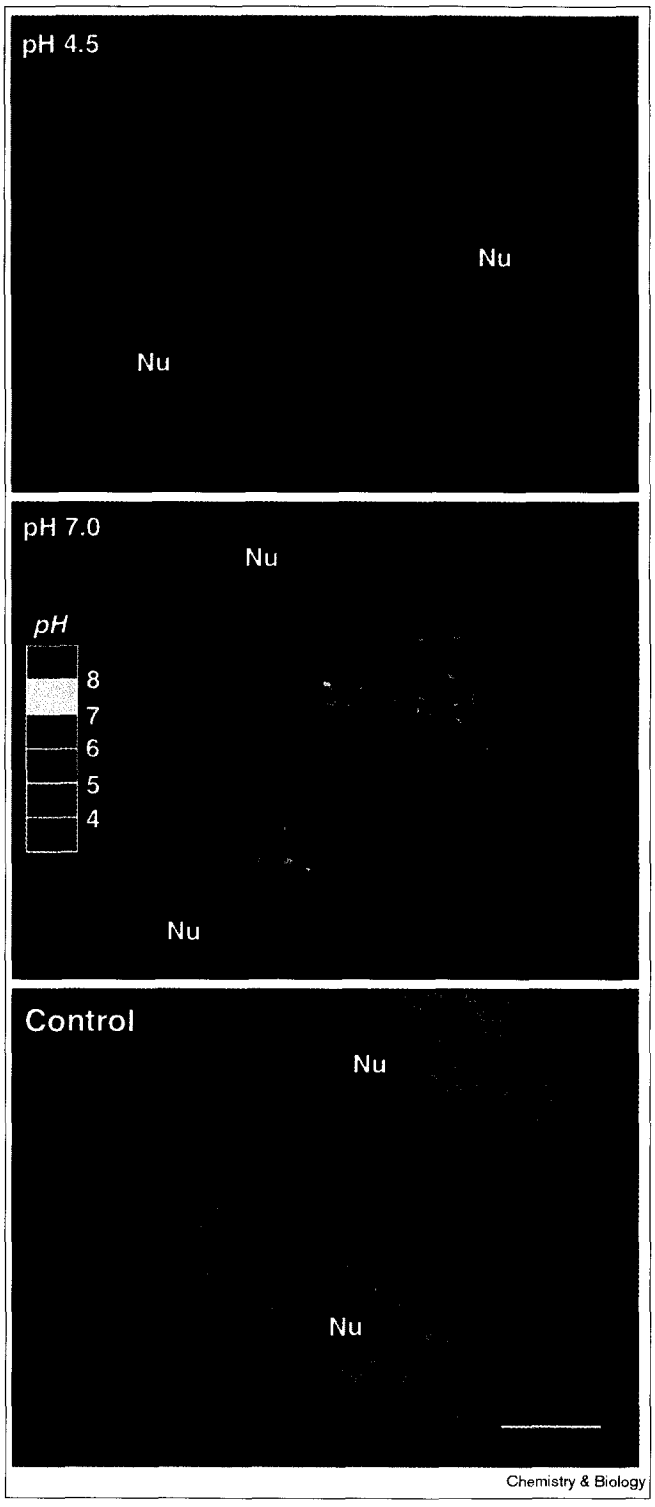

The pseudo-color ratio images of untreated and ionophore-treated MDCK cells stained with compound **8**. MDCK cells were treated with nigericin and monensin respectively in pH 4.5 and pH 7.5 buffers. The lysosomal pH of the controlled cells (untreated) was estimated to be 4.4–4.5 using the standard pH calibration curve (Figure 4). Nu, nucleus; Scale bar, 10 μm.

'blue'/'green' emission increases as pH increases. The lysosomal pH of the control MDCK cells (untreated) was estimated to be 4.4–4.5 using the standard pH calibration curve (Figure 5). The emission ratio of PDMPO is quite sensitive to pH changes (up to pH 6.0) although the probe has a pK_a of 4.47 (see above). It has been proven that excitation and emission ratio changes of ratiometric fluorescent probes are much more sensitive to the surrounding environment than their intensity changes [18]. Ratio imaging has been shown to have many advantages over intensity-based imaging. For example, errors in fluorescence measurements resulting from leakage, photobleaching, cell thickness and nonuniform dye distributions can be corrected using excitation or emission ratios [18].

The dual excitation of BCECF has been widely used to determine the pH of various biological systems [7,29]. Dual excitation methods are not readily adaptable to techniques such as flow cytometry and laser scanning microscopy, however, which often employ a single excitation wavelength [18]. DHPN has been used as an emission-ratio-imaging intracellular pH indicator. Unfortunately, the dye fails to exhibit a true isosbestic point, indicating that more than two fluorescent species might be involved in the multiple equilibria [11]. Additionally, both BCECF and DHPN show greatly reduced fluorescence in acidic medium [15]. PDMPO shows clear pH-dependent wavelength shifts in both excitation and fluorescence with well-behaved isosbestic points. The large separation of the two distinct peaks in both excitation and emission make the selection of wavelengths for ratio measurements quite flexible. It must be emphasized, however, that R, R_{max} and R_{min} are very sensitive to the wavelengths chosen and also to individual instrumental characteristics such as the intensity profile of the light source, the excitation bandwidth and the photomultiplier sensitivity [18]. In actual applications, the indicator must be calibrated under the conditions to be used for experimental pH measurement.

Significance

Changes in intracellular pH play an important role in many cellular events. For this reason many techniques have been developed to measure intracellular pH. Fluorescence spectroscopy has greater sensitivity than most methods and fluorescent pH indicators have been developed to monitor these changes. Most of these pH probes, however, are ill adapted for studying acidic organelles such as lysosomes and endosomes. We set out to develop probes that can be used in ratio imaging that are strongly fluorescent even in acidic media.

2-(4-pyridyl)-5-((4-(2-dimethylaminoethylaminocarbamoyl)methoxy)phenyl)oxazole (PDMPO) is shown to be a convenient fluorescent probe that can be used to selectively label lysosomes of live cells. The two distinct spectral peaks of PDMPO in both its excitation and emission

can be readily explored to monitor the lysosomal pH fluctuations of live cells (in ratio measurements) and to study the biosynthesis and pathogenesis of the lysosomes (such as lysosomal storage diseases) [26,30,31]. Additionally, the very large Stokes shift and excellent photostability of PDMPO make the compound an ideal fluorescent acidotropic probe. The unique fluorescence properties of PDMPO might give researchers a new tool with which to study acidic organelles of live cells. We believe that PDMPO analogs with higher pK_a values will useful for investigating several other types of acidic compartments such as *trans*-Golgi vesicles [32], endosomes [12] and subpopulations of coated vesicles in fibroblasts [33], spermatozoa acrosomes and plant vacuoles [8]. Such probes are currently under development and will be reported in due course.

Materials and methods

Equipment and chemicals

Absorption and fluorescence spectra were recorded on an Aminco SPE-5000 and an Aminco SPF-500C spectrophotometer respectively. NMR spectra were obtained on a Bruker YLIV370.040. Melting points were measured on a Mel-Temp II apparatus (Laboratory Devices, Inc., Holliston, MA) and are uncorrected. All the solvents (spectral grade) and 2,5-diphenyl-oxazole (DPO) were purchased from Aldrich Chemical Company (Milwaukee, WI), and used without further purification. Penicillin, streptomycin, monensin and gentamicin were purchased from Sigma Chemical Company (St. Louis, MO). Nigericin is the product of Molecular Probes, Inc. (Eugene, OR). Compounds **2–7** were synthesized analogously to the procedure of Diwu *et al.* [22], and the NMR spectra confirm their structures. Compounds **9**, **11** and **12** were prepared according to the protocol of Kauffman *et al.* [34]. Compounds **8** and **10** were prepared as described below.

*Synthesis of PDMPO (compound **8**)*

Compound **7** (470 mg, 1.6 mmol) and *N*-hydroxysuccinimide (376 mg, 2.4 mmol) were dissolved in anhydrous tetrahydrofuran (50 ml). To the solution was added dicyclohexylcarbodiimide (490 mg, 2.4 mmol) in three portions. The resulting solution was stirred at room temperature until compound **7** was completely dissolved. *N,N*-dimethylethylenediamine was added dropwise to the reaction mixture. The resulting solution was stirred at room temperature overnight. The reaction mixture was concentrated under high vacuum to ~2 ml, and the residue was poured into ether (100 ml). The precipitate was collected by filtration and washed with ether (3 × 100 ml). The crude solid was further purified on a silica gel column to give a pale yellow solid using a gradient mixture of chloroform and methanol as eluant. The solid was recrystallized from ethyl acetate to give the pure desired product (480 mg, yield: 82%). m.p. 141–142°C. ^{1}H-NMR ($CDCl_3$): 8.26 (2H, dd, J = 8 Hz); 7.92 (2H, dd, J = 8 Hz); 7.68 (2H, dd, J = 12 Hz); 7.43 (1H. s); 7.02 (1H, m, D_2O exchangeable); 7.01 (2H, dd, J = 12 Hz); 4.56 (2H, s); 3.40 (2H, m); 2.45 (2H, m); and 2.27 ppm (6H, s). λ_{max} (ε) in methanol: 331 nm (23488 $cm^{-1}M^{-1}$).

*Synthesis of compound **10***

Compound **9** (200 mg, 0.8 mmol) and 1,3-propanesultone (212 mg, 1.8 mmol) were dissolved in 1,2-dichlorobenzene (5 ml). The resulting solution was refluxed until compound **9** was completely dissolved and then cooled to room temperature. The resulting precipitate was collected by filtration and washed with ether (3 × 100 ml). The crude solid was recrystallized from ethyl acetate to give the pure desired product (261 mg, yield: 87%). m.p. > 300°C. ^{1}H-NMR (DMSO-d_6): 9.18 (2H, dd, J = 11 Hz); 8.63 (2H, dd, J = 11 Hz); 8.09 (1H, s); 7.94 (2H, dd, J = 12 Hz); 7.12 (2H, dd, J = 12 Hz); 4.77 (2H, m); 3.36 (2H, m); and 2.48 ppm (2H, m). λ_{max} (ε) in methanol: 405 nm (21486 $cm^{-1}M^{-1}$).

Spectral analysis

Absorption and fluorescence spectra were obtained using 5 μM and 0.5 μM of dye concentrations, respectively. Titration samples were prepared in 50 mM potassium phosphate buffers of the appropriate pH. The pH of each solution was measured at the time of spectrophotometric analysis. Extinction coefficients were determined by standard Beer's law calculations. All measurements, unless otherwise specified, were performed at ambient temperature.

The fluorescence quantum yields were determined using quinine sulfate in 5 M H_2SO_4 as the reference standard ($\Phi_F = 0.55$) [35]. The concentrations of the reference and test compounds were adjusted to have the same absorbance (0.05 in a 1 cm cell) at the peak wavelength of the test compounds (Table 1), which were used as excitation wavelength. Under these conditions, the fluorescence quantum yield of the test compound (Φ_F^X) was calculated from the following equation [22], considering that the peak area (A_R) of the emission spectrum of the reference and that of the tested dye (A_X) can be readily determined:

$$\Phi_F^X = A_x \Phi_F^R / A_R \qquad (2)$$

where Φ_F^R and Φ_F^X are the fluorescence quantum yields of the reference and the test dye. The measurements were carried out in triplicate and the estimated errors were no more than 1%.

Lysosomal staining

Mock cells (MDCK, CCL-34, American Type Culture Collection, MD), were routinely grown in a monolayer (30%–50% confluence) on a glass cover slide at 37°C in DMEM (Dulbecco's Modified Eagle Medium), supplemented with 1% L-glutamine, 1% HEPES (4-(2-hydroxyethyl)piperazine-1-(2-ethanesulfonic acid)), 0.5% gentamicin, 1% penicillin/streptomycin and 10% fetal bovine serum. At the time of the experiment, the cells were incubated with 5 μM of compound **8** in RPMI-1640 medium (RPMI supplemented with 1% L-glutamine and penicillin/streptomycin, Gibco, NY) at 37°C for 5 min. Excess dye was removed with cold phosphate buffer saline (PBS) washing. Labeling of lysosomes with Texas Red-conjugated dextran was performed as previously described [28,36]. Briefly, cell monolayer was pulse-labeled with the complete culture medium containing 2 mg/ml of Texas Red-conjugated dextran (10K, Molecular Probes, Inc., OR) at 37°C for 18 h. The excess dye was then removed and cells were incubated in fresh medium at 37°C for another 2 h.

Fluorescence microscopy and image processing

Fluorescence microscopic experiments were performed with an inverted microscope (DIAPHOT-TMD, Nikon) equipped with a Planapo 60X (1.4 N.A.) objective and epifluorescence optics respectively for PDMPO and Texas Red fluorophores. For PDMPO, exciter is BP357–373 nm, dichroic is 400 nm, emitter is BP490–530 nm for green images and BP417–483 nm for blue images. The Texas Red optics consists of an exciter of BP540–560 nm, a dichroic of 595 nm and an emitter of BP600–620 nm. A CCD camera (Quantix, Photometrics Ltd., AR) was used to obtain the microscopic images.

For quantitative microscopic experiments, PDMPO-stained cells were excited with attenuated UV light (357–373 nm), and observed in green (490–530 nm) and blue (417–483 nm) region of the spectra. Images of the same cell were collected first in the green and then in the blue channel. Images of blank regions of the culture dish were acquired at both emission wavelengths and used to correct the background fluorescence as described previously [37]. Thirty-two fluorescence video images of PDMPO-treated cells were digitized (16 bits) and calculated using the MetaMorph Image processing system (Universal Imaging Corp., PA).

To obtain a pH calibration curve, cells were treated with 10 μM monensin and 10 μM nigericin and equilibrated for 2 min with MES (4-morpholineethanesulfonic acid) calibration buffer solutions containing 5 mM NaCl, 115 mM KCl, 1.2 mM $MgSO_4$ and 25 mM MES (pH from

4.0 to 7.5) prior to image acquirement [38]. The fluorescence emission intensity ratio of blue/green in the lysosomal region was calculated and processed according to the procedure of Chen *et al.* [37].

References

1. Martínez-Zaguilán, R., *et al.* & Gillies, R.J. (1996). [Ca^{2+}] and pH homeostasis in Kaposi sarcoma cells. *Cell Physiol. Biochem.* **6**, 169-184.
2. Satoh, H., Hayashi, H., Katoh, H., Terada, H. & Kobayashi, A. (1995). Na^+/H^+ and Na^+/Ca^{2+} exchange in regulation of [Na^+] and [Ca^{2+}] during metabolic inhibition. *Am. J. Physiol. Heart Circ. Phy.* **37**, H1239-H1248.
3. Nuccitelli, R. (1994). *A Practical Guide to the Study of Calcium in Living Cells.* Vol. 40, Academic Press, San Diego, USA.
4. Okamoto, C.T. (1998). Endocytosis and transcytosis. *Adv. Drug Deliv Rev.* **29**, 215-228.
5. Falke, J.J., Bass, R.B., Butler, S.L., Chervitz, S.A. & Danielson, M.A. (1997). The two-component signaling pathway of bacterial chemotaxis: a molecular view of signal transduction by receptors, kinases, and adaptation enzymes. *Ann. Rev. Cell Dev. Biol.* **13**, 457-512.
6. Shimizu, Y. & Hunt III, S.W. (1996). Regulating integrin-mediated adhesion: one more function for PI 3-kinase? *Immunol. Today* **17**, 565-573.
7. Tsien, R.Y. (1989). Fluorescent indicators of ion concentrations. In *Fluorescence Microscopy of Living Cells in Culture.* (Taylor, D.L. ed.), Vol. 30, Part B, pp. 127-156, Academic Press, San Diego, USA.
8. Haugland, R.P. (1996). *Handbook of Fluorescent Probes and Research Chemicals* (6th ed.), Molecular Probes, Inc., Eugene, Oregon, USA.
9. Johnson, I. (1998). Fluorescent probes for living cells. *Histochem. J.* **30**, 123-140.
10. Warner, I.M., Soper, S.A. & Mcgown, L.B. (1996). Molecular fluorescence, phosphorescence, and chemiluminescence spectrometry. *Anal. Chem.* **68**, R73-R91.
11. Czarnik, A.W. (1995). Desperately seeking sensors. *Chem. Biol.* **2**, 423-428.
12. Overly, C.C., Lee, K.D., Berthiaume, E. & Hollenbeck, P.J. (1995). Quantitative measurement of intraorganelle pH in the endosomal lysosomal pathway in neurons by using ratiometric imaging with pyranine. *Proc. Natl Acad. Sci. USA* **92**, 3156-3160.
13. Sandhu, V., Miller, M. & Grover, A.K. (1998). Effects of peroxide on the fluorescence of the Ca^{2+} probe Fluo-3 and the pH probe BCECF. *Mol. Cell Biochem.* **178**, 77-80.
14. Devoisselle, J.M., Soulie, S., Mordon, S. & Maillols, H. (1996). Fluorescent characteristics and pharmacokinetic profiles of the fluorescent probe BCECF in various tissues: the role of blood content. *Photochem. Photobiol.* **64**, 906-910.
15. Liu, J.X., Diwu, Z.J. & Klaubert, D.H. (1997). Fluorescent molecular probes III. 2′,7′-*bis*-(3-carboxypropyl)-5-(and-6)-carboxyfluorescein (BCPCF): a new polar dual-excitation and dual-emission pH indicator with a pKa of 7.0. *Bioorg. Med. Chem. Letter* **7**, 3069-3072.
16. Whitaker, J.E., Haugland, R.P. & Prendergast, F.G. (1991). Spectral and photophysical studies of benzo[c]xanthene dyes: dual emission pH sensors. *Anal. Biochem.* **194**, 330-344.
17. Kneen, M., Farinas, J., Li, Y. & Verkman, A.S. (1998) Green fluorescent protein as a noninvasive intracellular pH indicator. *Biophys J.* **74**, 1591-1599.
18. Bright, G.R., Fisher, G.W., Rogowska, J. & Taylor, D.L. (1989). Fluorescence ratio imaging microscopy. *Methods Cell. Biol.* **30**, 157-192.
19. Martínez-Zaguilán, R., Seftor, E.A., Seftor, R.E.B., Chu, Y.W., Gillies, R.J. & Hendrix, M.J.C. (1996). Acidic pH enhances the invasive behavior of human melanoma cells. *Clin. Exp. Metastasis* **14**, 176-186.
20. Anderson, R.G.W. & Orci, L. (1988). A view of acidic intracelluar compartments. *J. Cell Biol.* **106**, 539-543.
21. Holtzman, E. (1989). *Lysosomes.* Plenum Press, New York, USA.
22. Diwu, Z., Lu, Y.X., Zhang, C.L., Klaubert, D.H. & Haugland, R.P. (1997). Fluorescent molecular probes .2. The synthesis, spectral properties and use of fluorescent solvatochromic Dapoxyl™ dyes. *Photochem. Photobiol.* **66**, 424-431.
23. King, L.C. & Ostrum, G.K. (1964). Selective bromination with copper(II) bromide. *J. Org. Chem.* **29**, 3459-3461.
24. deSilva, A.P., Gunnlaugsson, T. & Rice, T.E. (1996). Recent evolution of luminescent photoinduced electron transfer sensors – a review. *Analyst* **121**, 1759-1762.
25. Babcock, D.F. (1983). Examination of the intracellular ionic environment and of ionophore action by null point measurements employing the fluorescein chromophore. *J. Biol. Chem.* **258**, 6380-6389.
26. Reeves, J.P. (1984). The mechanism of lysosomal acidification. In *lysosomes in biology and pathology.* (Dingle, J.T., Dean, R.T. & Sly, W. ed.), Vol. 7, pp. 175-199, Elsevier, Amsterdam, The Netherlands.
27. Wang, Y.X., Shi, L.B. & Verkman, A.S. (1991). Functional water channels and proton pumps are in separate populations of endocytic vesicles in toad bladder granular cells. *Biochemistry*, **30**, 2888-2894.
28. Koval, M. & Pagano, R.E. (1990). Sorting of an internalized plasma membrane lipid between recycling and degradative pathways in normal and Niemann-Pick, Type A fibroblasts. *J. Cell Biol.* **111**, 429-442.
29. Wang, X.F. & Herman, B. (1996). *Fluorescence Imaging Spectroscopy and Microscopy.* John Wiley & Sons, New York, USA.
30. Galjarrd, H. & Reuser, A.J.J. (1984). Genetic Aspects of Lysosomal Storage Diseases. *in Lysosomes in Biology and Pathology.* (J.T. Dingle ed.), Vol. 7, pp. 315-379, Elsevier, Amsterdam, The Netherlands.
31. Tassin, M., Lang, T., Antoine, J., Hellio, R. & Ryter, A. (1990). Modified lysosomal compartment as a carrier of slowly and non-degradable tracers in macrophages. *Europ. J. Cell Biol.* **52**, 219-228.
32. Anderson, R.G.W. & Pathak, R.K. (1985). Vesicles and cisternae in the trans Golgi apparatus of human fibroblasts are acidic compartments. *Cell* **40**, 635-643.
33. Barasch, J., Kiss, B., Prince, A., Saiman, L. & Gruenert, D. (1991). Defective acidification of intracellular organelles in cystic fibrosis. *Nature* **352**, 70-73.
34. Kauffman, J.M., Litak, P.T. & Adams, J.K. (1992). Syntheses and photophysical properties of some 5(2)-aryl-2(5)-(4-pyridyl)oxazoles and related oxadiazoles and furans. *J. Heterocylic Chem.* **29**, 1245-1273.
35. Demas, J.N. & Crosby, G.A. (1971). The measurement of photoluminescence quantum yields. a review. *J. Phys. Chem.* **75**, 991-1024.
36. Chen, C.-S., Rosenwald, A.G. & Pagano, R.E. (1995). Ceramide as a modulator of endocytosis. *J. Biol. Chem.* **270**, 13291-13297.
37. Chen, C.-S., Martin, O.C. & Pagano, R.E. (1997). Changes in the spectral properties of a plasma membrane lipid analog during the first seconds of endocytosis in living cells. *Biophys. J.* **72**, 37-50.
38. Bronk, S.F. & Gores, G.J. (1991). Efflux of protons from acidic vesicles contributes to cytosolic acidification of hepatocytes during ATP depletion. *Hepatology* **14**, 626-633.

Because *Chemistry & Biology* operates a 'Continuous Publication System' for Research Papers, this paper has been published via the internet before being printed. The paper can be accessed from http://biomednet.com/cbiology/cmb – for further information, see the explanation on the contents pages.